Non-Gaussian diffusion weighted imaging for assessing degenerative changes in intervertebral disc composition

Masaki Katsura[1,2], Yuichi Suzuki[2], Akihiro Kasahara[2], Harushi Mori[1], Akira Kunimatsu[1], Yoshitaka Masutani[3], Masaaki Hori[4], Shigeki Aoki[4], and Kuni Ohtomo[1]

[1]Radiology, Graduate School of Medicine, The University of Tokyo, Tokyo, Japan, [2]Radiology, The University of Tokyo Hospital, Tokyo, Japan, [3]Intelligent Systems, Hiroshima City University, Hiroshima, Japan, [4]Radiology, School of Medicine, Juntendo University, Tokyo, Japan

Introduction: The intervertebral disc (IVD) consists of the nucleus pulposus (NP) in the core and the annulus fibrosus (AF) at the periphery [1]. It has been known that IVDs undergo structural and morphological changes throughout the various stages of development and aging [2]. Degeneration of IVDs has been implicated as a major etiologic component of lower back pain [3]. Diffusion-weighted imaging (DWI) has been applied for the quantification of IVD degeneration as the apparent diffusion coefficient (ADC) [4, 5], and is expected to reflect microstructural changes such as matrix composition (water, proteoglycan, and collagen) and matrix integrity. Conventional DWI analysis is based on an assumption that the water molecules follow a Gaussian distribution. However, human tissue including the IVD is a complex and restricted environment that hinders the distribution of water molecules, resulting in distributions that are far from Gaussian [6]. Q-space imaging (QSI) analysis is a more advanced form of diffusion analysis. In contrast to conventional DWI, QSI does not assume a Gaussian shape for the underlying probability density function (PDF) of water molecule diffusion [7]. QSI has shown promise for evaluating the microstructure of tissues in vivo because it can provide additional diffusion metrics, namely the root mean square displacement (RMSD) and apparent kurtosis coefficient (AKC) [8-11], which give in vivo microstructural information that complements the ADC values. We therefore hypothesized that QSI analysis would be able to provide more information about degenerative changes in the microstructural complexity in IVDs.

Purpose: To investigate the use of RMSD and AKC metrics of QSI data for assessing IVD degeneration.

Methods: We investigated 7 male subjects with lower back pain. None of the subjects had previous spine surgery, major systemic disease, serious illness (e.g. tumor, infection), or spinal fractures. Images were acquired using 3 Tesla MR (Signa HDx ver. 14.0; General Electric). After routine fast spin-echo (FSE) T2-weighted sagittal and axial imaging, QSI and T2 mapping data were acquired in the axial plane of the IVD between the fourth and fifth lumbar vertebrae (L4/5 disc). FSE T2-weighted images were not only used for anatomical reference but for the visual Pfirrmann grading of IVDs [12]. QSI was performed by using a spin-echo diffusion weighted echo-planar imaging sequence with the following parameters: TR: 5000 [ms]; TE: 99.6 [ms]; NEX: 3; FOV: 25.6 [cm]; matrix size: 128 x 128; slice thickness: 4.0 [mm]; and 11 b values (0, 40, 160, 360, 640, 1000, 1440, 1960, 2560, 3240, 4000 [s/mm^2]) with diffusion encoding in three directions for every b value. Gradient length (δ) and the time between the two leading edges of the diffusion gradient (Δ) were 33.9 and 39.9 ms, respectively. A multiecho spin echo sequence was performed for T2 mapping data acquisition with the following parameters: TR: 1200 [ms]; TE: 7.9, 15.8, 23.8, 31.7, 39.6, 47.5, 55.4, 63.4 [ms]; NEX: 0.5; FOV: 22 [cm]; matrix size: 256 x 256; slice thickness: 5.0 [mm]. For post-processing, QSI analyses were performed using the free software Volume-One 1.72 (http://www.volume-one.org/) and dTV II FZR (http://www.ut-radiology.umin.jp/people/masutani/dTV.htm). T2 maps were created with Functool software (Advantage Windows Workstation, General Electric), and T2 values were measured using the free software Image J (/rsbweb.nih.gov/ij/). Five equally sized circular regions of interest (ROIs) on the central slice of the axial plane (Fig. 1) were manually drawn. Each ROI (4 - 6 mm) measured 20% of the midline disc diameter in the axial plane. The most anterior and most posterior ROIs (ROI 1 and ROI 5) were interpreted as anterior and posterior AF, respectively. The ROIs in between were interpreted as NP (ROI 2, anterior NP; ROI 3, middle NP; ROI 4, posterior NP). The subjects were classified into two groups: (1) normal-appearing or mildly degenerated IVDs (Pfirrmann grade 1 & 2); (2) advanced degenerated IVDs (Pfirrmann grade 3-5). Student t-tests were applied for assessing significant differences in T2 and diffusion values (ADC, RMSD, and AKC) between the two groups. A P value < 0.05 was considered to be significant.

Fig 1: Positioning of the regions of interest

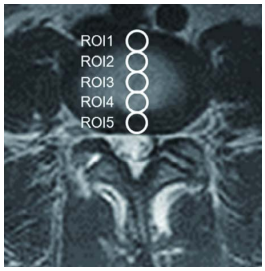

Table 1: Demographic characteristics of subjects

	Group 1 (n=3)	Group 2 (n=4)	P
Age (years)	30.2 ± 5.2	33.5 ± 6.8	0.31
BMI (kg/m^2)	21.1 ± 2.0	21.9 ± 0.7	0.51

Results: There were 3 subjects in group 1 ("Pfirrmann grade 1 & 2") and 4 subjects in group 2 ("Pfirrmann grade 3-5"). Demographic characteristics are shown in Table 1 (presented as mean ± standard deviation [SD]). There were no significant differences for age and body mass index (BMI) between the two groups. T2, ADC, RMSD, and AKC values within each ROI are shown in Tables 2-5. In the NP (ROIs 2-4), T2, ADC, and RMSD values of group 2 were significantly lower ($p<0.05$) when compared to those of group 1. In contrast, the AKC values of group 2 were significantly higher ($p<0.05$), when compared to those of group 1. No significant differences were observed between the two groups in the AF (ROIs 1 & 5).

Table2: T2 values (msec)

	Group 1	Group 2	p
ROI 1	74.6 ± 6.5	65.3 ± 12.6	0.30
ROI 2	166.7 ± 43.0	77.8 ± 22.4	**0.02**
ROI 3	219.1 ± 69.9	84.3 ± 21.7	**0.01**
ROI 4	144.6 ± 41.2	74.5 ± 9.4	**0.02**
ROI 5	55.3 ± 8.5	62.5 ± 5.2	0.22

Table3: ADC values (10^{-3}mm^2/s)

	Group 1	Group 2	P
ROI 1	0.66 ± 0.09	0.68 ± 0.18	0.85
ROI 2	1.24 ± 0.12	0.86 ± 0.18	**0.02**
ROI 3	1.57 ± 0.06	0.97 ± 0.31	**0.02**
ROI 4	1.26 ± 0.10	0.80 ± 0.26	**0.03**
ROI 5	0.66 ± 0.10	0.61 ± 0.08	0.45

Table 4: RMSD values (μm)

	Group 1	Group 2	p
ROI 1	24.7 ± 0.6	25.1 ± 0.8	0.48
ROI 2	43.5 ± 4.3	28.7 ± 2.6	**<0.01**
ROI 3	49.3 ± 2.7	30.5 ± 5.5	**<0.01**
ROI 4	42.5 ± 1.2	26.7 ± 1.9	**<0.01**
ROI 5	25.8 ± 0.9	25.4 ± 0.6	0.51

Table 5: AKC values

	Group 1	Group 2	p
ROI 1	2.78 ± 0.37	2.56 ± 0.38	0.49
ROI 2	0.60 ± 0.07	1.34 ± 0.34	**0.02**
ROI 3	0.53 ± 0.03	1.34 ± 0.48	**0.03**
ROI 4	0.62 ± 0.03	1.89 ± 0.72	**0.03**
ROI 5	2.79 ± 0.73	2.63 ± 0.41	0.73

Discussion: Our results showed decreased RMSD values and increased AKC values in the NP regions of IVDs with higher Pfirrmann grades (group 2), compared with those with lower Pfirrmann grades (group 1). Water molecule diffusion is restricted in a complex manner by several factors such as extracellular matrix (e.g. collagen fibers and proteoglycan). In general, RMSD is not influenced by the viscosity of water, but by the space for free water movement. AKC describes the deviation of the water diffusion pattern within a voxel from a Gaussian distribution, which is thought to reflect the changes in microstructural complexity. Our results suggest that the degenerative process of IVDs involves narrowing of the space for free water movement and a generally higher degree of microstructural complexity.

Conclusion: The RMSD and AKC values obtained from QSI analysis may be sensitive biomarkers for IVD degenerative microstructural changes in which we are unable to assess with conventional diffusion-weighted imaging metrics based on an assumption of a Gaussian shape and model of water molecules.

References: [1] Mwale F et al. Eur Spine J 2008:17:432–440. [2] Gruber HE et al. Spine 2002:27:798–805. [3] Luoma K et al. Spine 2000:25:487–492. [4] Niu G et al. AJNR 2011:32:1617–23. [5] Zhang W et al. Eur Spine J 2014:23:1830-6. [6] Kärger J. Adv Colloid Interface Sci 1985:23:129–148. [7] Callaghan PT et al. Nature 1991:351:467–469. [8] Assaf Y et al. Magn Reson Med 2002:47:115–126. [9] Farrell JA et al. Magn Reson Med 2008:59:1079–1089. [10] Hori M et al. Acad Radiol 2011:18:837–841. [11] Hori M et al. Eur Radiol 2012:22:1797–1802. [12] Pfirrmann CW et al. Spine 2001:26:1873–1878.